MLF Experimental Report	提出日 Date of report 2014 年 10 月 11 日
実験課題番号 Project No. 2012S01 実験課題名 Title of experiment 高分解能チョッパー分光器による物質のダイナミクスの研究 実験責任者名 Name of principal investigator 伊藤晋一、佐藤卓* 所属 Affiliation 高エネルギー加速器研究機構、東京大学*	装置責任者 Name of responsible person 伊藤晋一 装置名 Name of Instrument/（BL No.） HRC (BL12) 利用期間 Dates of experiments 2012 年 4 月 － 2013 年 3 月

1．研究成果概要（試料の名称、組成、物理的・化学的性状を明記するとともに、実験方法、利用の結果得られた主なデータ、考察、結論、図表等を記述してください。

Outline of experimental results (experimental method and results should be reported including sample information such as composition, physical and/or chemical characteristics.

1. Overview

The High Resolution Chopper Spectrometer (HRC) is being operated at BL12 in MLF, J-PARC, to study dynamics in condensed matters with high-resolutions and relatively high-energy neutrons. We report here the activity of the S-type project on the basis of the HRC in FY2012 (2012S01). This project is aim to establish a comprehensive picture in condensed matter physics by observing wide range of electron correlated systems using the HRC. We selected some topics among them and focused on the following four points of view: novel ground states in low dimensional quantum spin systems, interactions among spin, charge, orbital and lattice in electron systems with strong or medium electron- correlations, origin of magnetism in ferromagnetic metals, magnetism related to characteristic structures in strongly correlated electron systems. We performed experiments concerning these subjects, as described below.

For this purpose, the HRC was improved. In particular, the neutron Brillouin scattering (NBS) experiments on the HRC became feasible by the improvement of the collimation of the incident neutron beam [1]. The NBS is the inelastic neutron scattering in the forward direction, and therefore, this is effective to observe ferromagnetic spin waves from polycrystalline samples. The development of the NBS method on the HRC is described in a separate section in this report.

The element strategy project conducted by the MEXT started in 2012 and the IMSS became one of key institutes for this project. The aim of this project is to develop functional materials without rare elements. Preliminary experiments on a strong permanent magnet $Nd_2Fe_{14}B$ as a magnetic material and an Fe-based superconductor as an electronic material were performed on the HRC, as a project of the IMSS.

The HRC has accepted experiments for the general use since 2011B. In FY2012, five general use experiments were performed: successive metal- nonmetal transitions with totally-symmetric electron ordering in $(Pr_{1-x}Ce_x)Ru_4P_{12}$ (part I) by K. Iwasa, confirmation of spin gap excitations in the large-spin substances $RCrGeO_5$ (R = Y or Nd) by M. Hase, high-energy inelastic neutron scattering on $NiGa_2S_4$ by Y. Nambu, successive metal-nonmetal transitions with totally-symmetric electron ordering in $(Pr_{1-x}Ce_x)Ru_4P_{12}$ (part II) by K. Iwasa, and, proton entangled sates in double hydrogen bond system by S. Ikeda.

2. Instrumentation

NBS experiments on the HRC became feasible by the improvement of the beam collimation. The computer environment was also improved for the data analysis and the instrument control, and some other developments were performed.

A collimator system was installed just upstream of the sample in order to reduce background noise. The divergence of the incident neutron beams is controlled by the collimator, which composed of slits of vertical cadmium sheets. The collimators having the collimation of 0.3° and 1.5° are mounted in the collimator system, one of the two can be selected by an elevation mechanism with a motor control. On the HRC, position sensitive detectors (PSD) are mounted at the scattering angles ϕ = 3 – 42° for conventional inelastic neutron scattering experiments, the background noise for these experiments was successfully reduced by using the 1.5° collimator. Also, on the HRC, PSDs are mounted at low angles down to ϕ = 0.5°, the 0.3° collimator can reduce the background in this low angle part. This 0.3° collimator is effective for NBS.

The computer environment composes of the data analysis software and the experiment control platform. The data analysis software was improved in the following points: The intensity normalization process for the inelastic neutron scattering from powder samples was improved, the analyzed data were transformed to the standard Mslice format for a convenience of users, and the process for the alignment of the sample crystal became very easy. The experiment control platform was also improved, and therefore, almost all the hardwares on the HRC can be controlled from the computer terminal and these operations can be connected with the data acquisition (begin/end of running). In addition, a conceptual design for the analysis software and the experiment control platform was performed towards the improvement plan in next year.

For conventional inelastic neutron scattering experiments, 128 pieces of 2.8m-PSDs, which are mounted into two detector banks, covers ϕ = 3 – 42° at present. PSDs for the next detector bank werepurchased, and we will install them next year. The cryopump is being operated for the high vacuum in the scattering chamber. The algorithm of the regeneration process of the cryopump was improved. The scattering chamber and its vacuum system were installed in 2009. The maintenance work for them was performed. In particular, the normal property of the large thin Al window on the surface of the chamber, which was designed on the assumption of a finite lifetime due to permitting the plastic defor mation of the window, was confirmed. In order to cool the sample down to 4 K stably, a GM-type refrigerator was installed. Since the cadmium slits were successful for the incident beam collimator, an oscillating radial collimator was manufactured for the collimation of the scattered neutron beam. The performance will be investigated soon. The deck connecting the space of BL12 to the mezzanine was constructed, and therefore, the mezzanine in the 1st experimental hall was completed.

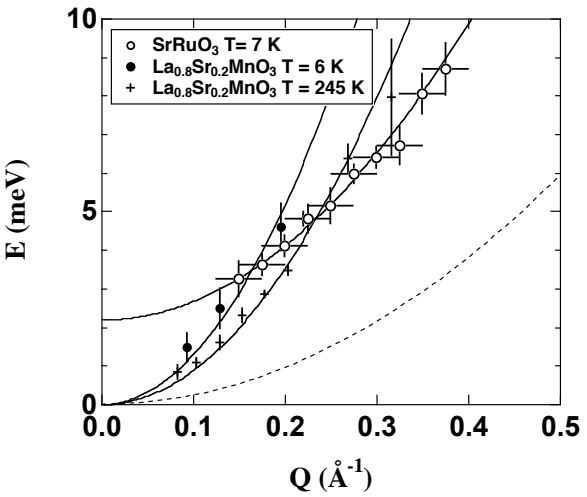

Fig.1 Spin-wave dispersion curves for $La_{0.8}Sr_{0.2}MnO_3$ and $SrRuO_3$ determined on the HRC. The solid lines are fitted curves. The dashed line is the upper boundary accessible with a conventional spectrometer.

必要に応じて、A4 サイズの用紙に続きを記入して下さい。
Please use A4-size papers for further reporting, if necessary.

3. Neutron Brillouin Scattering Experiments

On the HRC, the NBS experiments became feasible by reducing the background noise at low scattering angles down to $\phi = 0.5°$. NBS is the most promising way to observe excitations in the forward direction from powders, polycrystals, or liquids. Owing to the kinematical constraints of neutron spectroscopy, incident neutron energy (E_i) in the sub-eV region is necessary for measuring scattering in the meV transferred energy (E) range close to (000), and with a high energy resolution of $\Delta E/E_i$, further, the scattered neutrons need to be detected at very low scattering angles (ϕ). Low angle detectors are essential to access the present energy momentum space. In fact, the region above the dashed line in Fig. 1, which is the envelope of scan loci for $\phi = 5°$ with respect to E_i, can never be accessed using a conventional spectrometer with the lowest scattering angle of $\phi = 5°$, for instance.

First, NBS experiment was performed on the HRC to observe spin waves in a polycrystalline sample of a cubic perovskite, $La_{0.8}Sr_{0.2}MnO_3$, (Curie temperature: $T_C = 316$ K). Magnetic properties of this material are well elucidated and it has been already reported that spin waves were measured by using a single crystal sample. Figure 1 shows the dispersion relation of spin waves in $La_{0.8}Sr_{0.2}MnO_3$ measured with $E_i = 100$ meV, where $\Delta E/E_i = 2\%$. The observed dispersion relations at 6 and 245 K were well fitted to $E = DQ^2$, where Q is the scattering vector. The D values were obtained to be 130 ± 13 and 88 ± 2 meVÅ^2 at 6 and 245 K, respectively. These values are in good agreement with the results (D = 131 and 89 meVÅ^2 at 14 and 250K, respectively) obtained by the previous inelastic neutron scattering experiments using a single crystal [2,3]. Therefore, the feasibility of NBS experiments on the HRC was demonstrated [1].

Next, spin waves in a polycrystalline ferromagnet, $SrRuO_3$ (T_C = 165 K), were similarly measured. This material also has a cubic perovskite structure, but a large single crystal suitable for inelastic neutron scattering experiments has not yet been synthesized. The measurement was performed at 7 K with $E_i = 100$ meV, and well-defined spin wave peaks were observed. As shown in Fig. 1, the dispersion relation of spin waves in $SrRuO_3$ was well fitted to $E = E_0 + DQ^2$ with an apparent energy gap E_0 [1]. This characteristic feature might originate from an induced spin anisotropy possibly from a spin-orbit coupling acting on the Ru 4d orbital. The anomalous Hall effect in $SrRuO_3$ was theoretically interpreted as a strong spin-orbit interaction [4].

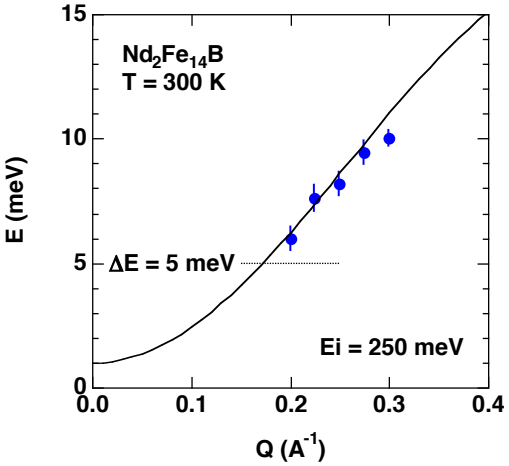

Fig. 2 Spin wave dispersion relation of $Nd_2Fe_{14}{}^{11}B$ observed on the HRC. The solid line is the dispersion curve along the *c*-axis determined using a single crystal sample

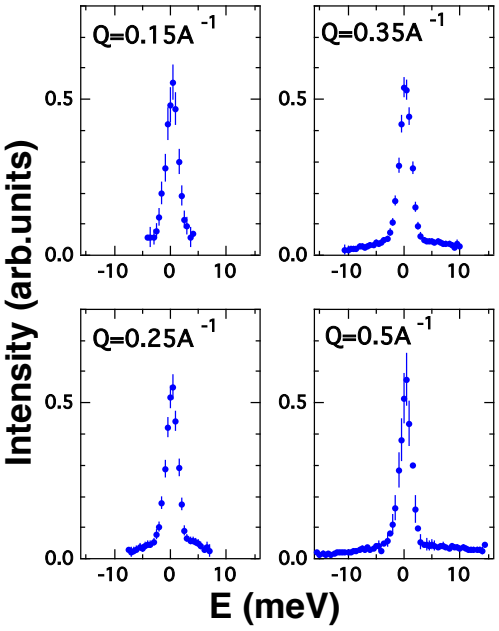

Fig. 3 Inelastic scattering spectra for liquid D_2O. The broad spectra beside the elastic scattering are acoustic phonons.

A strong permanent magnet $Nd_2Fe_{14}B$ shows demagnetization at high temperatures. Recovery of magnetization at high temperatures is possible by adding Dy, which is the rare element. One of the aims in the element strategy project is to develop Dy-free magnet. Before development, evaluation methods of materials should be established. We measured spin waves in $Nd_2Fe_{14}{}^{11}B$ polycrystals at 300 K and 6 K with E_i = 250 meV. As shown in Fig. 2, assuming there exists a spin wave peak in the observed range, the peak positions are just on the dispersion relation along the *c*-axis determined by the previous single crystal experiment [5]. To determine interaction parameters from these data, theoretical supports are required.

Acoustic phonons in liquid D_2O were observed. It was reported, previously, the observation of broad spectra with E_i = 80 meV and ΔE = 4.8 meV and the determination of the dispersion relation of the acoustic phonons [6]. We measured with E_i = 100 meV and ΔE = 2 meV with a better resolution and with a wider energy range. Similar spectra to the previous data were obtained with a slightly wide energy- momentum space, as shown in Fig. 3.

4. Experiments and Results

4.1 Search of Orbital Waves in YVO_3

The orthorhombic perovskite YVO_3 shows the G-type orbital ordering in the temperature range from 200 to 77 K [7]. In this phase, the existence of large orbital fluctuations is suggested [8], and dispersive orbital waves propagating along the *c*-axis, due to the one-dimensional spin-orbital correlations, is predicted [9]. In consideration of the neutron scattering cross-section obtained from the correlation function for the orbital angular moment, we have attempted to detect the orbital waves. Figure 4 shows observed spectra in the orbital ordered phase (133 K), subtracted from those in the orbital disordered phase (214 K). The intensity decreases with increasing $|\boldsymbol{Q}|$, where $\boldsymbol{Q} = h\boldsymbol{a}^* + k\boldsymbol{b}^* + l\boldsymbol{c}^*$, which can be explained by the magnetic form factor for the V^{3+} orbital. In addition, we found the intensity shows a periodic behavior with the maximum at l = odd number. This indicates that the observed spectra are originated from the orbital waves. This experiment was performed using the fine-resolution Fermi-chopper spectrometer, SEQUOIA at SNS, ORNL, as one of the substituted proposals for the disaster of the earthquake on 11 March 2011.

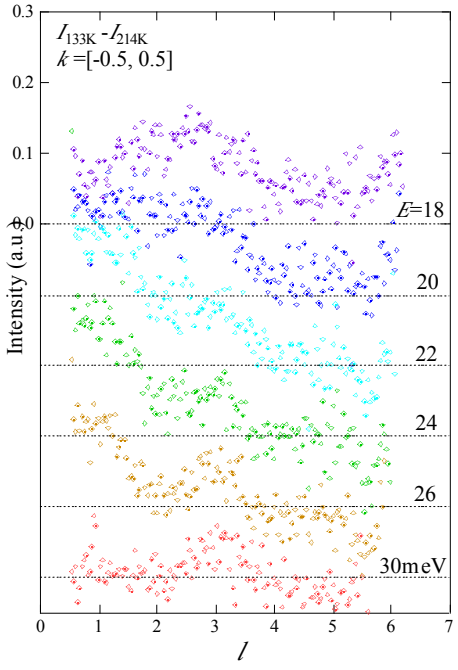

Fig. 4 Inelastic neutron spectra in the orbital ordered phase (133K), subtracted from that in the orbital disordered phase (214K). The horizontal axis l is the propagating direction of the predicted orbital waves.

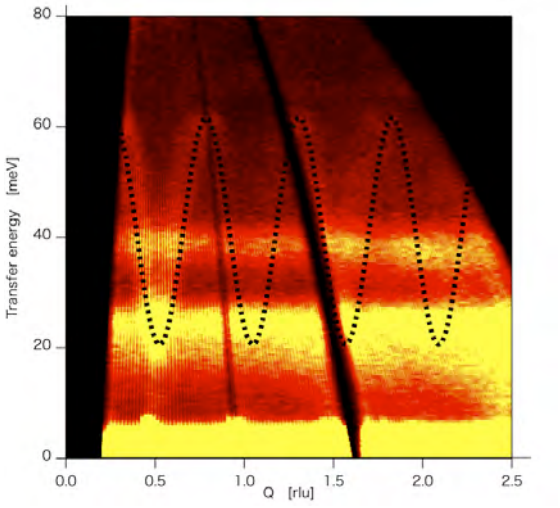

Fig. 5 Observed S(Q,E) spectrum of $Nd_{1.965}Ca_{0.035}BaNiO_5$.

4.2 Mind the "Gap" on Quantum Spin Systems

Quantum spins in low-dimensional system show unusual quantum phases such as Haldane system and spin-Peierls state, by strong quantum nature. In particular, spin singlet is the basic starting point describing a ground state of the quantum spin chain. Another interest in a quantum spin systems is the cooperation among physical degrees of freedoms. The strong correlations between quantum spin and charge, orbital, and lattice are expected to give rise to a fascinating new quantum phase as a realization of high-T_c superconductivity in two-dimensional system.

1) Finding the Gap in TiOBr ~ A Novel Spin- Peierls System? ~: Newly proposed spin-Peierls system TiO*X* (*X*: Cl, Br) has been revealed showing one-dimensional (1D) nature associated with orbital ordering of Ti ions and super-lattice structure being related to the Peierls instability. It is pointed out that resulting only from an arrangement of Ti d_{xy} orbital, the formation of 1D spin chains and the spin-Peierls transition will be realized. Recently, it has been demonstrated that TiOBr also exhibits two successive phase transitions similar to TiOCl at T_{c1}=27K and T_{c2}=47K. Inelastic neutron experiments were carried out in order to find the direct evidence of spin-Peierls transition, namely, the spin gap. The inelastic spectrum with a large amount of poly crystalline sample of TiOBr is expected to show the localized signal in the vicinity of the magnetic zone center Q=0.9Å^{-1}. This low-Q access measurement of poly crystalline sample is only done by small angle and high incident energy (E_i) condition. The detectors at around 3 degrees of scattering angle and 200 meV of E_i are used for searching the excitation at low-Q region. However, obtained $S(Q,E)$ shows no indication of the existence of magnetic signals in the spectrum except for phonon contribution. The gap energy in TiOBr is expected much higher from that measured thermodynamic properties and by analogy with TiOCl, and could be 20 meV in energy. It still remains as open questions if the spin-Peierls state under the cooperation of orbital ordering is realized in this system.

2) Hole Dynamics in a 1D Spin Chain: It is practically hard to realize the carrier doping in 1D material because the localization of carriers occurs at low temperature. We tested spin and hole dynamical properties in $Nd_{2-x}Ca_xBaNiO_5$, which is successfully hole doped 1D Haldane system. The lightly doped x=0.035 carrier content were measured by means of pulsed neutron inelastic scattering as shown in Fig. 5. It is clearly observed the entire one-magnon band with spin gap (Haldane gap) at magnetic zone center (MZC) addition to intense crystal field excitation of Nd ions. The energy at zone boundary reaches 60 meV that is less comparing to undoped Haldane chain. On the other hand, the gap slightly increases in its energy, but still gap opens even holes doped (spin correlation of Haldane state is known to be spatially exponential). Moreover, new dynamical structures within the Haldane gap were observed upon carrier doping, showing incommensurate structures centered at MZC. This is originated by the dynamics of doped-holes. For further experiments, hole carrier dependence of Ni chain band (Haldane band) and hole dynamics will be focused.

4.3 Multiferroic Compounds

RFe$_3$(BO$_3$)$_4$ (R=rare earth metal) are a series of multiferroic compounds that crystallize trigonal structure with three fold screw chains of FeO$_6$ octahedra and R^{3+} ions along the crystallographic c direction. In R=Nd compound easy-plane type Néel order and spontaneous electric polarization appear simultaneously at T_N=30K. Weiss temperature is -115 K and the frustration ratio is -3.8. Thus the compound exhibits multiferroic property as well as the behavior of frustrated magnet. While magnetic structure was studied in detail [10], magnetic excitation was measured only by using electro- magnetic wave including ESR and Raman scattering techniques. Inelastic neutron scattering (INS) experiment to measure the $S(\mathbf{q},\omega)$ in wide $\mathbf{q}$ space is the most effective method to identify the spin Hamiltonian realized in the compound. 22 pieces of single crystals are coaligned by X-ray Laue camera so that a^*-c^* plane is the scattering plane. Total mass of the sample for INS experiment is 2.1g. T0 chopper is set at 50Hz, 1.5° of collimator is installed in front of sample, and Fermi chopper, "S", with 200Hz is used to obtain high neutron flux. GM-type refrigerator was used to achieve 15 K. Figure 6 (a) shows the spectrum obtained at the configuration of k_i parallel to the crystallographic a^* direction. Flat mode at $\hbar\omega$ ~ 1meV is crystal field excitation of Nd ion, which was consistently observed by ESR and Raman scattering experiment [11,12]. The dispersive modes at 2.5 meV < $\hbar\omega$ < 4.5 meV have not been identified yet but it would be possibly originated from collective spin wave excitation from Fe^{3+} ions. Figure 6 (b) is the spectrum of k_i parallel to the c^* direction. In addition to the modes observed in Fig. 6 (b), dispersive mode with anisotropy gap of 0.5 meV is observed. The anisotropy energy scale is consistent with those of Fe^{3+} system observed in ESR experiment [11]. In the fiscal year of 2013 we will collect the $S(\mathbf{q},\omega)$ in wide $\mathbf{q}$ space by rotating crystals to identify the spin Hamiltonian realized in this compound.

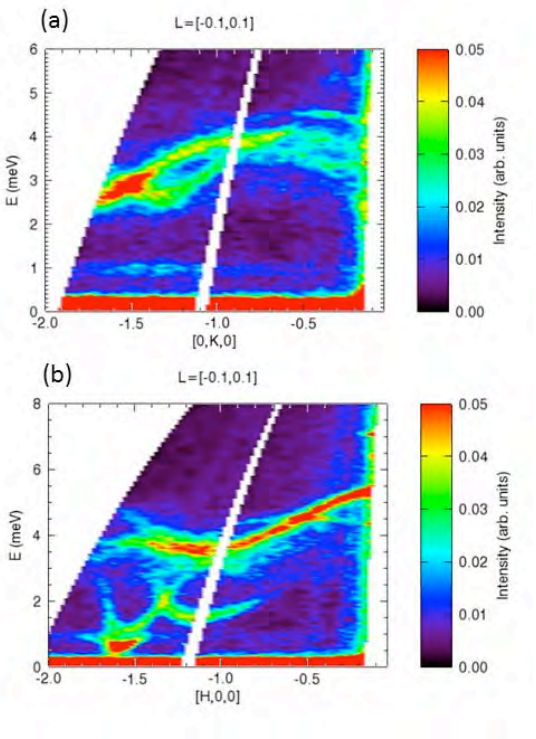

Fig. 6 Inelastic neutron scattering spectrum of $NdFe_3(BO_3)_4$ in case of k_i // a^* (a) and k_i // c^* (b).

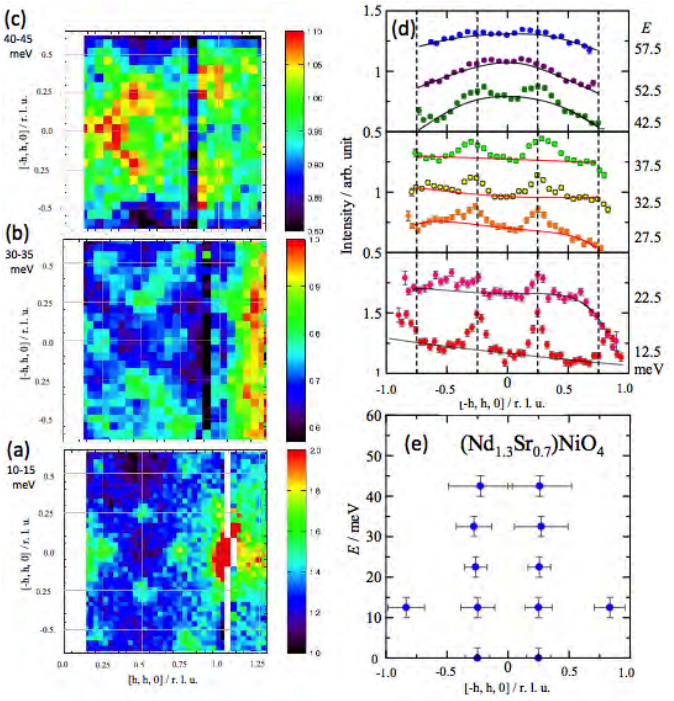

Fig. 7 Neutron-scattering measurements from $(Nd_{1.30}Sr_{0.70})NiO_4$ measured on HRC (BL12). (a) - (c) Constant energy slices showing the variation of the intensity in the (h, k) plane at different energies. The data are averaged over the range of energies indicated in the figure. (d) Constant energy cuts along [-H, H, 0] directions at various energies. The data are averaged over (H, H) = (1.0, 1.0) ± (0.1, 0.1). (e) Dispersion of the magnetic excitations in $(Nd_{1.30}Sr_{0.70})NiO_4$ along [-H, H, 0] direction.

4.4 Unusual Spin Dynamics in the Checkerboard Order in Two-Dimensional Layered Nickelate

When the antiferromagnetic insulating phase is melted by carrier doping in the layered transition- metal oxides, the hole doping stabilizes the non- trivial spin-charge ordering towards the metal- insulator transition. In particular, the doped carriers tend to form the stripe or simple square-lattice checkerboard patterns. Although the magnetic excitations in the insulating stripe phase region can be explained by the linear spin-wave approximation with in-plane magnetic anisotropic exchange parameters, a breakdown of the linear spin wave approximation was observed in the magnetic excitations in the checkerboard phase with higher carrier concentration. The spin dynamics in the checkerboard phase of $(La_{2-x}Sr_x)NiO_4$ (x = 0.5) and more metallic $(Nd_{2-x}Sr_x)NiO_4$ (x = 0.6, 0.7) are systematically investigated by inelastic neutron scattering experiment using a large single crystals grown by the floating-zone method. We found that the observed magnetic excitations in the checker- board phase is qualitatively different from those of the more insulating stripe phase. They do not show behavior of counter-propagating spin wave branches up to ΔE~ 70 meV as shown in Fig. 7 (a-e), but are rather similar to those in the high Tc cuprates which show straight-up chimney-like excitations.

4.5 Kagome Lattice Antiferromagnet

Geometrical frustrated systems with reduced spatial dimensionality have gathered considerable interest. They can suppress conventional magnetic orders, and eventually induce novel states of magnetism. Here we concentrate on Kagome lattice antiferromagnet (KAF), which composes of corner-sharing triangles. Since no candidate material of KAF with exact lattice geometry and strong two-dimensionality have so far been reported, low-temperature magnetism remains to be controversial. There have indeed reported several scenarios to describe magnetism of KAF in theories. One of intriguing subjects is if the excitation from nonmagnetic ground state to magnetic excited state is gapfull or gapless. We have recently examined a prominent example of S = 1/2

systems, $Rb_2Cu_3SnF_{12}$, and revealed the pinwheel valence bond solid ground state. In addition, an analogue $Cs_2Cu_3SnF_{12}$ with $S = 1/2$ is revealed to magnetically order into so-called $Q = 0$ structure. Through inelastic neutron scattering experiments, we successfully estimated coupling constants of spins. To gain further insight into detailed view of magnetic excitations of this compound, we performed an inelastic neutron scattering measurement on BL12 HRC. A single crystal is mounted on the (HHL) horizontal scattering plane and the (00L) was set to be parallel to the incident neutron beam. We measured spectra at $T = 5$ K using a CCR with $E_i = 81.9$ meV. Due to lack of sample mass and beam intensity, we were unable to obtain conclusive data and only phonon signals were observed at high-Q regime (Fig.8(a)). Owing to the multi-E_i system of HRC, however, we succeeded in detecting magnetic signals spanning G-point (2,2,0) to K-point (5/3,5/3,0) with $E_i = 21.8$ meV, which is good accord with recent results of triple-axis and BL14 AMATERAS spectrometers (Fig.8(b)). We will hereafter pursue its magnetic origin, and induce quantum critical phenomena by diluting such chemically analogous systems showing distinct low-temperature magnetism.

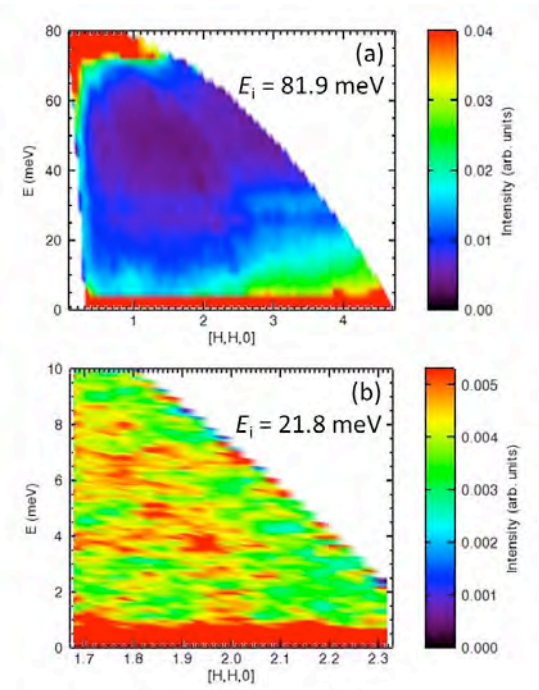

Fig. 8 Contour maps of intensity in $Cs_2Cu_3SnF_{12}$ as a function of energy and inplane wave vector for (a) E_i = 81.9 and (b) 21.8 meV. The intensity is integrated over the whole reachable range of (0,0,L) and (-K,K,0).

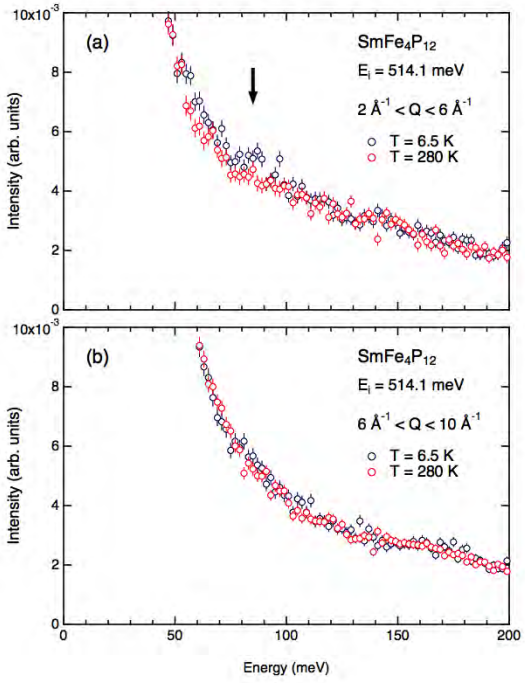

Fig. 9 Inelastic neutron spectra of $SmFe_4P_{12}$ at T = 6.5 K and 280 K for (a) momentum transfer range 2 Å^{-1} < Q < 6 Å^{-1} and (b) 6 Å^{-1}< Q < 10 Å^{-1}.

4.6 Intermultiplet Transition in Filled Skutterudite Compound $SmFe_4P_{12}$

Samarium-based filled skutterudite $SmFe_4P_{12}$ was reported to be the first ferromagnetic Kondo-lattice compound. It shows an unconventional heavy-electron state with the large electronic specific-heat coefficient 370 mJ/mol K^2 and a ferromagnetic transition at 1.6 K. Although the 4f electrons clearly have a key role in a formation of heavy quasiparticle at low temperatures, there has been lack of basic information about the 4f electronic states in this system because neutron scattering experiments on materials containing thermal neutron absorber elements such as Sm. To avoid this problem, thus we have done INS experiment on $SmFe_4P_{12}$ by using higher energy neutrons. Figure 9 shows the inelastic neutron spectra of polycrystalline $SmFe_4P_{12}$ at 6.5 K and 280 K. The sample was prepared by using a tin flux method, where natural abundant Sm isotopes were used. In low Q range, a small peak around 80 ~ 90 meV is observed at low temperature. This peak is not visible in high Q range, indicating that it is of magnetic origin. If this peak is associated with the intermultiplet transition from $J = 5/2$ ground state to $J = 7/2$ multiplet, interestingly, the energy splitting is very small compared to usual Sm-based compounds. This might originate from the strong c-f hybridization in filled skutterudite compounds.

4.7 Magnetic Excitations in Antiferromagnetic Alternating Spin-3/2 Chain Substance $SmCrGeO_5$

One interesting phenomenon in quantum spin systems is the appearance of a spin-singlet ground state with a spin gap (singlet-triplet excitation). When the spin value is larger than 1, existence of a spin-singlet ground state with a spin gap has not been proved experimentally. We can expect anti- ferromagnetic (AF) alternating spin-3/2 chains of Cr^{3+} in $SmCrGeO_5$ and a spin-singlet ground state with a spin gap. We performed inelastic neutron scattering experiments on $SmCrGeO_5$ powders to confirm the spin gap excitation. Excitations are apparent between 15 and 25 meV at 7.8 K. Intensities of the excitations are strong in the small Q range and decrease with increasing temperature. Therefore, most of excitations are magnetic excitations. We could confirm a spin gap in the magnetic excitations. Figure 10 shows the intensity map in the ω-Q_{1D} plane at 7.8 K obtained using the conversion method developed by Tomiyasu et al. The results correspond to results of a single crystal measured along the spin chain direction. The intensity is the strongest around Q_{1D} = 0.5 as expected in AF spin chains. The white line shows $\omega = \sqrt{13.8^2 sin^2(2\pi Q_{1D}) + 18.6^2}$. The spin gap value is estimated as 18.6 meV. The dispersion is apparent below Q_{1D} = 0.75.

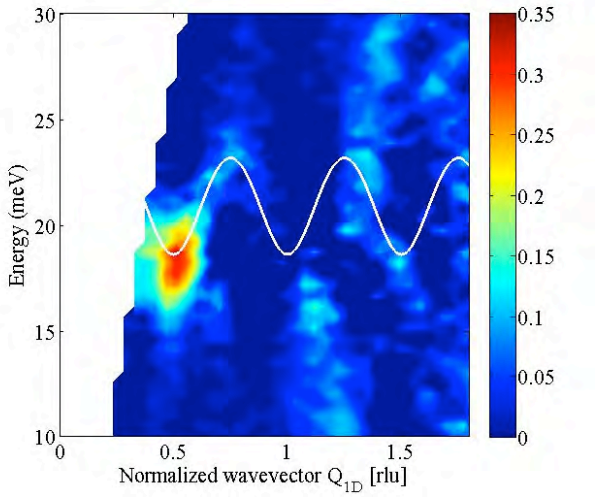

Fig.10 The intensity map in ω-Q_{1D} plane obtained from the data of $SmCrGeO_5$ at 7.8 K with E_i = 91.6 meV. Q_{1D} is Q parallel to the spin chain and is normalized by $2\pi/d$, where d is the Cr-Cr average distance (0.286 nm).

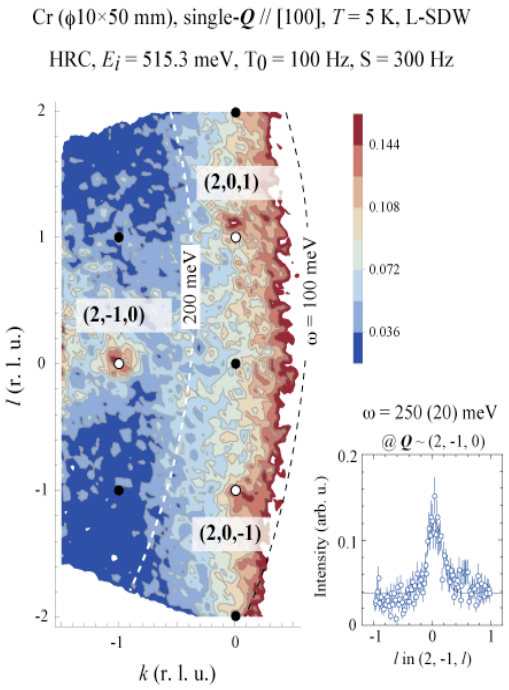

Fig. 11 Intensity contour onto (2, *k*, *l*) plane with a thickness of $1.9 \le h \le 2.1$. The inset shows a line cut profile along l at (2, -1, 0) integrating within a range of $1.9 \le h \le 2.1$ and $-1.1 \le k \le -0.9$.

4.8 Spin Density Waves in Chromium

The spin-density wave (SDW) in Cr is one of the most fascinating subjects in condensed matter physics. It has a history of long and continuing research. One of the open issues is its magnetic excitation, which arises from incommensurate magnetic Bragg positions with a steep dispersion slope and extends to more than 600 meV. In order to examine the detailed structure of high-energy magnetic excitations of Cr in ($\boldsymbol{Q}$, ω) space, we performed inelastic magnetic neutron scattering on HRC using a single crystal with 4 cc in volume. Figure 11 shows an intensity contour map in the longitudinally-spin-polarized SDW state, where the intensity is projected on (2, *k*, *l*) plane over a wide energy range. Sharp spots appears at three magnetic Γ points: (2, -1, 0) at ω = 250 meV, and (2, 0, ±1) at ω = 150 meV. The line-cutting profiles along *l* direction evince that the magnetic cross sections are well localized in $\boldsymbol{Q}$ space. No consensus has been established yet for this novel high-energy excitation. One scenario is based on spin-wave excitations from a pseudo localized-spin system with a zone-boundary energy of ~1 eV, though Cr is usually regarded as a typical itinerant-electron system. Another possibility comes from electron excitations across the Fermi energy, possibly reflecting the peculiar Fermi surfaces. Further experimental studies toward high-energy region are required not only to settle such the argument, but also to get a clue to unknown spin dynamics in metallic magnets.

4.9 Collective Dynamics of Hydrated β-Lacto- globulin

Protein hydration plays a fundamental role in protein behavior: water-protein interactions affect protein folding, maintain structural integrity, mediate molecular recognition, and accelerate enzymatic catalysis. Many scattering measurements, both elastic and inelastic, and many molecular dynamics simulations, have been performed to investigate the relation between protein dynamics and that of the surrounding solvent molecules. Single particle dynamics of proteins and hydrated water have been investigated using incoherent scattering from hydrogen in hydrated protein powder. On the other hand, the investigation of collective dynamics of proteins and hydrated water using coherent scattering is relatively scarce although it contains important information of structure and dynamics. First, we performed NBS experiment of pure D_2O at room temperature on HRC, as mentioned above. The fast sound mode due to the collective dynamics of water was detected as well as the inelastic X-ray scattering [13]. Next, hydrated β-lactoglobulin powder (water 0.4g/ dry protein g) was measured at 298 K -180K. The sample dimension was 40 x 40 x 8 mm. Figure 12 shows INS signals of the sample at different Q values. The spectra show well-defined acoustic excitations as shoulders (see arrows in the figure) that change in excitation energy with Q in the low Q region. This trend is similar to the results of hydrated ribonuclease A measured on BRISP (ILL) [14]. The analysis is in progress.

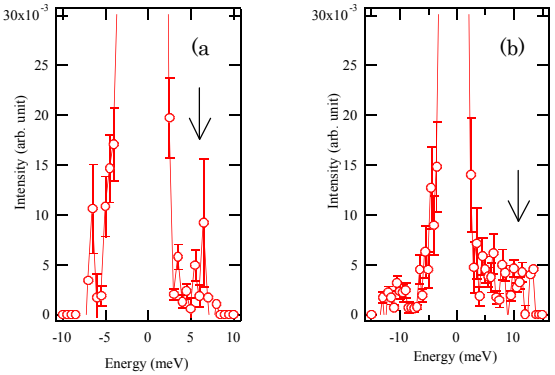

Fig. 12 Inelastic neutron spectra of hydrated β-lactoglobulin at 180 K for (a) momentum transfer range 2 $Å^{-1} < Q < 3$ $Å^{-1}$ and (b) 5 $Å^{-1} < Q < 6$ $Å^{-1}$.

References

[1] S. Itoh et al., J. Phys. Soc. Jpn. 82 (2013) 043001.
[2] F. Moussa et al., Phys. Rev. B 76 (2007) 064403.
[3] K. Hirota and Y. Endoh, J. Phys. Soc. Jpn. 66 (1997) 2264
[4] Z. Fang et al., Science 302 (2003) 92.
[5] H. M. Mayer et al., J. Magn. Magn. Mater. 97 (1991) 210.
[6] J. Teixeira et al., Phys. Rev. Lett. 55 (1985) 2681.
[7] S. Miyasaka et al., Phys. Rev. B 73 (2006) 224436.
[8] C. Ulrich et al., Phys. Rev. Lett. 91 (2003) 257202.
[9] S. Ishihara, Phys. Rev. B 69 (2004) 075118.
[10] M. Janoscheket et al., Phys. Rev. B 81 (201) 094429 .
[11] A.M. Kuz'menko et al., JETP Letters 94 (2011) 294.
[12] M.N. Popova, Phys. Rev. B 75 (2007) 224435.
[13] G. Ruocco et al., Nature 379 (1996) 521.
[14] A. Orecchini et al., J. Am. Chem. Soc. 131 (2009) 4664.